© 2020. Published by The Company of Biologists Ltd | Development (2020) 147, dev190124. doi:10.1242/dev.190124

RESEARCH ARTICLE

Hippo signaling promotes Ets21c-dependent apical cell extrusion in the *Drosophila* wing disc

Xianlong Ai, Dan Wang*, Junzheng Zhang and Jie Shen*

ABSTRACT

Cell extrusion is a crucial regulator of epithelial tissue development and homeostasis. Epithelial cells undergoing apoptosis, bearing pathological mutations or possessing developmental defects are actively extruded toward elimination. However, the molecular mechanisms of *Drosophila* epithelial cell extrusion are not fully understood. Here, we report that activation of the conserved Hippo (Hpo) signaling pathway induces both apical and basal cell extrusion in the *Drosophila* wing disc epithelia. We show that canonical Yorkie targets Diap1, Myc and Cyclin E are not required for either apical or basal cell extrusion induced by activation of this pathway. Another target gene, *bantam*, is only involved in basal cell extrusion, suggesting novel Hpo-regulated apical cell extrusion mechanisms. Using RNA-seq analysis, we found that JNK signaling is activated in the extruding cells. We provide genetic evidence that JNK signaling activation is both sufficient and necessary for Hpo-regulated cell extrusion. Furthermore, we demonstrate that the ETS-domain transcription factor Ets21c, an ortholog of proto-oncogenes *FLI1* and *ERG*, acts downstream of JNK signaling to mediate apical cell extrusion. Our findings reveal a novel molecular link between Hpo signaling and cell extrusion.

KEY WORDS: *Drosophila*, Hippo, Yorkie, Cell extrusion, JNK, Ets21c

INTRODUCTION

The Hippo (Hpo) pathway is conserved from *Drosophila* to mammals (Dong et al., 2007; Pan, 2010). Upstream key components of this pathway, including Hpo and Warts (Wts), form a core kinase cascade to regulate the transcriptional co-regulator Yorkie (Yki) (Huang et al., 2005; Kim et al., 2015; Praskova et al., 2008; Udan et al., 2003; Wu et al., 2003). When the Hpo pathway is inactive, dephosphorylated Yki is translocated into the nucleus and interacts with the DNA-binding transcription factor Scalloped (Sd) (Zhang et al., 2008). The Yki-Sd complex induces the expression of a wide range of target genes, including the *Cyclin E* (*CycE*) and *Myc* cell-cycle regulators, *bantam* (*ban*) microRNA and *Drosophila inhibitor of apoptosis protein 1* (*Diap1*) (Pan, 2010). Numerous studies have indicated that the Hpo pathway functions as a tumor suppressor. YAP1 (yes-associated protein 1, a Yki ortholog) is hyperactivated in some human cancers, including lung cancer (Wang et al., 2010) and uveal melanoma (Feng et al., 2014; Yu et al., 2014). However, YAP is also downregulated in individuals with multiple myeloma and in those with acute myeloid leukemia (Cottini et al., 2014).

Department of Entomology and MOA Lab for Pest Monitoring and Green Management, China Agricultural University, Beijing 100193, China.

*Authors for correspondence (shenjie@cau.edu.cn; dwang@cau.edu.cn)

D.W., 0000-0003-2881-2273; J.S., 0000-0002-6021-7151

Handling Editor: Thomas Lecuit
Received 4 March 2020; Accepted 28 September 2020

The Hpo pathway is essential for epithelial tissue development and homeostasis by regulating cell survival (Tapon et al., 2002), cell proliferation (Halder and Johnson, 2011), organ size (such as that of the *Drosophila* eye and thorax and the mouse liver) (Dong et al., 2007) and cell-cell adhesion (Schroeder and Halder, 2012). It has been reported that *yki* mutant clones grow poorly in the third instar larval wing disc (Qing et al., 2014). In addition to roles in apoptosis and cell proliferation, the Hpo pathway has recently been implicated in cell extrusion and invasion, which may help to explain the poor survival of *yki* mutant clones. Expression of *ykiRNAi* along the anterior-posterior (AP) boundary of *Drosophila* wing discs induces cell migration across the AP boundary and basal cell extrusion (BCE) (Ma et al., 2017). However, except for apoptosis-induced BCE, whether cell extrusion causes the abnormal Hpo-Yki signaling-induced poor recovery rate is unclear.

In both invertebrate and vertebrate models, cell extrusion plays an important role in epithelial homeostasis and development as well as in cancer cell metastasis (Eisenhoffer et al., 2012; Gu and Rosenblatt, 2012; Gudipaty and Rosenblatt, 2017; Marinari et al., 2012; Ohsawa et al., 2018). Moreover, extruded tumor cells have invasive abilities (Dunn et al., 2018; Pagliarini and Xu, 2003; Shen et al., 2014; Vaughen and Igaki, 2016). Here, we tested the hypothesis that the Hpo pathway maintains tissue homeostasis by suppressing cell extrusion. We found that Hpo pathway activation, by repressing *yki* or expressing *hpo* or *wts*, induced both apical cell extrusion (ACE) and BCE. Furthermore, *ban* expression could suppress BCE but not ACE. We further demonstrated that JNK signaling was necessary and sufficient to induce ACE downstream of Yki. Mechanistically, we present genetic evidence that ACE induced by the Hpo-JNK pathway is mediated by Ets21c, a member of the ETS-domain transcription factor family.

RESULTS

Activation of the Hpo pathway induces cell extrusion

This study was designed to investigate whether poor *yki* mutant clone growth is due to the effect of cell extrusion, in addition to cell death and proliferation constriction. We used mosaic analysis with a repressible cell marker (MARCM) (Lee and Luo, 2001) to generate GFP-marked *yki* mutant clones and monitored their cellular behavior. Compared with the control clones (Fig. S1A,F), wing pouch *yki* mutant clones were rare and small (Fig. S1B,F). Next, we generated *UAS-ykiRNAi* and *UAS-GFP* co-expressing clones using flp-out technology (Harrison and Perrimon, 1993). After 72 h of growth, *ykiRNAi* clonal cells showed poor survival (Fig. S1C,D,G). Given that Yki is a cell death suppressor (Huang et al., 2005), the loss of clones may be caused by apoptosis. To address this possibility, *p35*, encoding a baculovirus pan-caspase inhibitor (Hay et al., 1995), was co-expressed with *ykiRNAi* in the clonal cells to suppress potential apoptosis. However, even when apoptosis was suppressed by *p35* expression, *ykiRNAi* clones were still very small and rare, especially in the wing pouch (Fig. S1E,G). Therefore, the

Development (2020) 147, dev190124. doi:10.1242/dev.190124

low recovery rate of clones lacking Yki activity was not due to apoptosis. These results support the possibility of cell extrusion in *yki* mutant clones.

To check whether cells with downregulated *yki* are extruded from the wing disc, vertical wing disc sections were examined by *y-z* scanning on a confocal microscope. The apical side of disc proper (DP) cells faces the lumen of the wing sac, and their basal side is the external surface, which contacts the hemolymph. We used Discs large 1 (Dlg1) (Knust and Bossinger, 2002) as an apical maker of the epithelia during *y-z* scanning. Compared with wild-type clones (Fig. 1A), *yki* mutant clones were rare and invaded into the lumen (Fig. 1B, arrow). *ykiRNAi* clones were rare and were extruded either basally or apically (Fig. 1C,D). To overcome the low recovery rates during clonal analysis, *UAS-ykiRNAi* was expressed under the control of a pan-disc-specific driver *C765-Gal4* (Fig. S2A,A′). There were two stripe regions close to the wing hinge folds with greatly reduced Dlg1 staining in the apical wing disc confocal sections when we decreased *yki* expression (two white circles in Fig. S2A′). We inspected the wing disc vertical section and found cells undergoing ACE when *yki* was silenced, and most of the apically extruded cells were located in the two regions with reduced Dlg1 staining (Fig. 1E,F, arrow). At the same time, BCE was also evident (Fig. 1E,F, arrowhead). ACE and BCE were observed in over 90% of the wing discs (Fig. S3A,C). We confirmed that the same ACE and BCE phenotypes were observed using another, independent, *UAS-ykiRNAi* line (Fig. S2B).

Hpo and Wts suppress Yki in the *Drosophila* wing disc (Huang et al., 2005). To confirm that activated Hpo signaling regulates cell extrusion, we inspected the vertical sections of wing discs expressing *hpo* and *wts*. Consistently, both ACE and BCE were observed in more than 95% of *UAS-hpo*-expressing wing discs (Fig. 1G; Fig. S3). Both ACE and BCE were observed in the *UAS-wts*-expressing wing disc pouch at high frequency (76.5% and 100% for ACE and BCE, respectively; n=34) (Fig. 1H; Fig. S3). These results suggest that the activated Hpo pathway induces both ACE and BCE in *Drosophila* wing discs. The absence of *yki* expression induces apoptosis (Huang et al., 2005), and this was confirmed by anti-cleaved-caspase-3 staining (Fig. S4A). Vertical sections showed that most of the dying cells were located either in the lumen or at the basal side of the epithelia (Fig. S4A). To examine

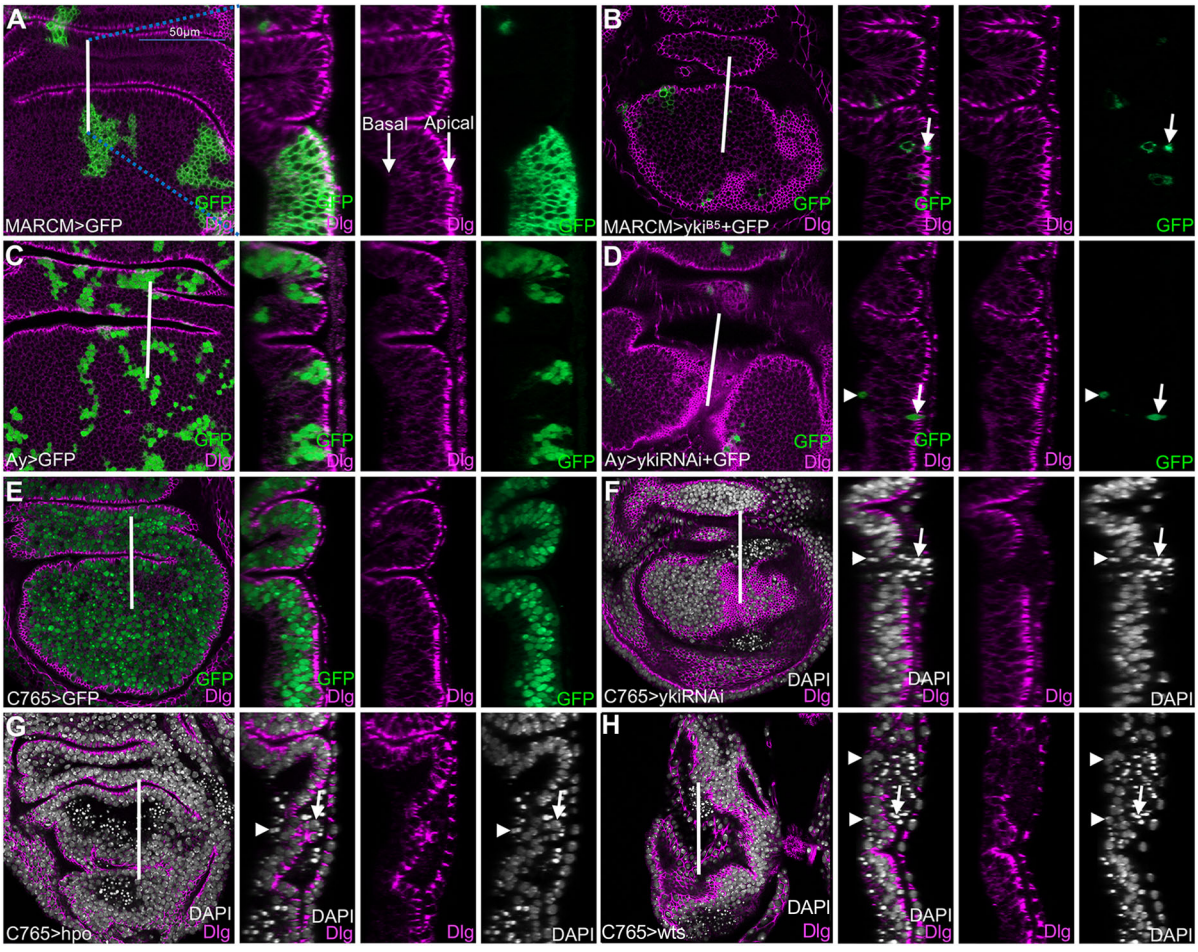

Fig. 1. Hpo pathway activation induces ACE and BCE. (A-H) The developmental stage of the wing imaginal discs shown in this and subsequent figures was middle to late 3rd instar. To better observe the apically located cells, *x-y* images of apical sections of the epithelia (left-hand images) were scanned by confocal microscopy. *y-z* images (panels on right) were scanned at the position indicated by white straight lines and are oriented with the dorsal side towards the top and the apical side to the right. Dlg1 staining was used to determine the apical side of the wing epithelia. Arrows indicate ACE and arrowheads indicate BCE, unless indicated otherwise. The *yki*-depleted line used was *UAS-ykiRNAi*^{THU0579}, unless indicated otherwise. (A) *GFP* control clones generated using the MARCM system. (B) MARCM system-generated *yki*^{B5} mutant clones were rare and tended toward apical extrusion (arrow). (C) *GFP* control clones generated using the flp-out system with *act5c>CD2>Gal4; UAS-GFP*. (D) *ykiRNAi* clones were rare and tended to undergo apical extrusion (arrow) or basal extrusion (arrowhead). (E) *GFP*-expressing cells driven by *C765-Gal4* were not extruded. (F-H) Cells expressing *ykiRNAi* (F), *hpo* (G) or *wts* (H) were extruded into the lumen (arrows) and to the basal side of the epithelia (arrowheads).

Development (2020) 147, dev190124. doi:10.1242/dev.190124

whether ACE and BCE are induced as a side effect of apoptosis, we co-expressed *p35* and *ykiRNAi*. Both ACE and BCE still occurred (Fig. S4B,C) at high frequency in clones co-expressing *p35* and *ykiRNAi* (74.2%, *n*=31) (Fig. S3A,C). These data indicate that cell extrusion induced by Hpo pathway activation is independent of apoptosis.

The Yki pathway target *ban* mediates BCE

We next tested whether canonical Hpo-Yki target genes mediate the observed cell extrusion. We checked four targets downstream of Yki: *Cyclin E* (*CycE*), a cell cycle regulator (Tapon et al., 2002); *Diap1*, an apoptosis inhibitor (Wu et al., 2003); *ban*, a microRNA that promotes growth and inhibits cell death (Nolo et al., 2006; Thompson and Cohen, 2006); and *Myc*, a crucial cellular growth effector (Neto-Silva et al., 2010). Co-expressing *ban* and *ykiRNAi* still induced ACE (Fig. 2A,B) at a high frequency (70%, *n*=30) (Fig. S3A,C), but the frequency of BCE in wing discs was reduced (16.7%, *n*=30). Co-expressing *Diap1* (Fig. 2C,D), *Myc* (Fig. 2E,F) or *CycE* (Fig. 2G,H) with *ykiRNAi* had little effect on ACE and BCE frequencies (Fig. S3A,C). These results suggest that BCE induced by silencing *yki* is largely dependent on *ban*, but ACE induced by silencing *yki* is not dependent on the canonical Hpo-Yki targets examined.

Transcriptional profiles upon *yki* manipulations in the wing disc

To further investigate the mechanism of ACE induced by *ykiRNAi*, we performed RNA-seq analysis in *ykiRNAi*-expressing wing discs. In *C765>ykiRNAi* versus *C765>* samples, we identified 833 transcripts with more than a 1.2-fold change in expression [false discovery rate (FDR) less than 0.05], including 500 upregulated genes and 333 downregulated genes (Fig. 3A,B; Table S1). Kyoto Encyclopedia of Genes and Genomes (KEGG) pathway analysis of the 833 transcripts revealed the enrichment of many pathways, including Hpo (Table S2) and JNK pathways (Fig. 3C). In the *Drosophila* wing disc, ACE is associated with tumor growth and invasion (Dunn et al., 2018; Tamori et al., 2016; Vaughen and Igaki, 2016), indicating that genes involved in these processes are potentially related to the ACE observed. By comparing our RNA-seq data with that produced through analyzing invasive tumors in *Drosophila* wing discs (Atkins et al., 2016), we found 90 genes that overlapped (Fig. 3E; Table S1). Gene ontology (GO) analysis suggested that these 90 genes were enriched in carbohydrate metabolic processes, salivary gland cell autophagic cell death, cellular response to gamma radiation, epithelial cell development and other developmental processes (Fig. 3F). Enrichment of carbohydrate metabolic processes indicates the need for macromolecule biosynthesis to support tumor growth

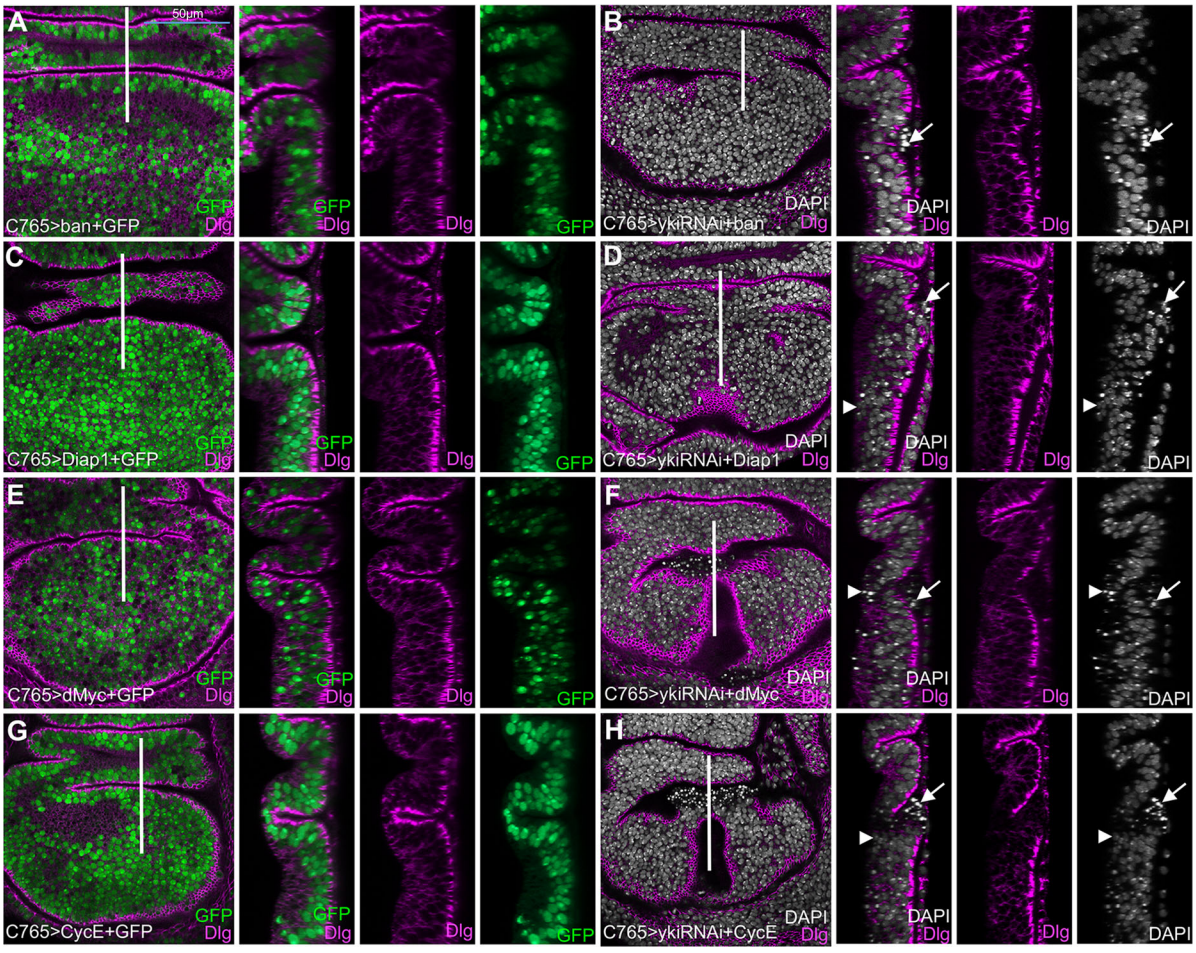

Fig. 2. *ban* mediates BCE, but canonical Hpo-Yki targets do not mediate ACE. (A-H) Images of wing imaginal discs are presented as described for Fig. 1. Arrows indicate ACE, arrowheads indicate BCE. (A) Control experiment showing *ban* expression. (B) Co-expression of *ban* and *ykiRNAi* did not prevent ACE induced by *ykiRNAi*, but did prevent BCE induced by *ykiRNAi*. (C) Control experiment showing *Diap1* expression. (D) BCE induced by *ykiRNAi* was not prevented by co-expressing *Diap1*. (E) Control experiment showing *Myc* expression. (F) BCE induced by *ykiRNAi* was not prevented by co-expressing *Myc*. (G) Control experiment showing *CycE* expression. (H) BCE induced by *ykiRNAi* was not prevented by co-expressing *CycE*. White vertical lines in the *x-y* section images (left) show the location of the *y-z* images.

Development (2020) 147, dev190124. doi:10.1242/dev.190124

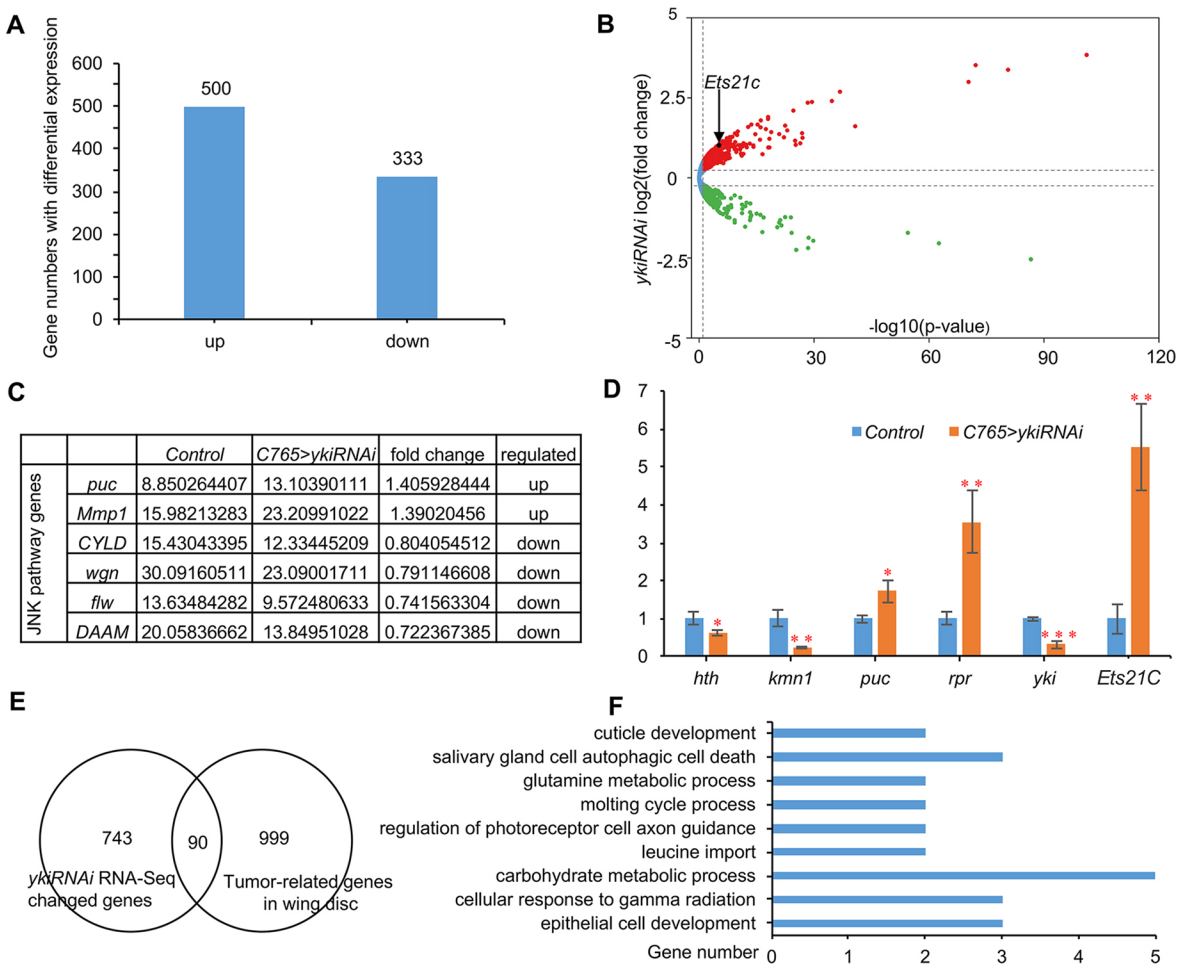

C

		Control	C765>ykiRNAi	fold change	regulated
JNK pathway genes	puc	8.850264407	13.10390111	1.405928444	up
	Mmp1	15.98213283	23.20991022	1.39020456	up
	CYLD	15.43043395	12.33445209	0.804054512	down
	wgn	30.09160511	23.09001711	0.791146608	down
	flw	13.63484282	9.572480633	0.741563304	down
	DAAM	20.05836662	13.84951028	0.722367385	down

Fig. 3. Profile of *ykiRNAi*-induced gene expression changes. (A) Bar chart showing the genes with altered expression in *ykiRNAi* wing discs, including 500 upregulated genes and 333 downregulated genes. (B) Distribution of fold change and significance for genes with altered expression, black arrow points to *Ets21c*. (C) mRNA expression alterations in six genes involved in the JNK pathway. (D) Four genes with altered expression (*hth*, *Kmn1*, *puc* and *rpr*), plus *yki* and *Ets21c*, were selected and subjected to RT-qPCR. n=3 (biological replicates). The change trends observed in the RT-qPCR data were similar to those seen in the transcriptome data. Results are shown as mean+s.d. *P* values were calculated using the paired two-tailed Student's *t*-test. **P*<0.05; ***P*<0.01; ****P*<0.001. (E) Venn diagram showing that 90 genes are present in both the set of genes shown in A and genes with changed expression in wing disc tumors (Atkins et al., 2016). (F) Some of these 90 genes were enriched in distinct functional GO clusters.

(Külshammer et al., 2015). Enrichment in salivary gland cell autophagic cell death and cellular response to gamma radiation terms reflects increased apoptosis. To further verify our RNA-seq results, *yki*, *Ets21c* and another four genes [*Kmn1*, *puckered* (*puc*), *rpr* and *hth*] were selected and their mRNA expression levels tested using RT-qPCR (reverse transcription quantitative real-time PCR). Consistent with the transcriptomic data, RT-qPCR results indicate that in the *yki*RNAi wing discs *hth*, *Kmn1* and *yki* were downregulated, whereas *puc*, *rpr* and *Ets21c* were upregulated (Fig. 3D; Table S3). We noticed that the expression levels of several JNK pathway components were altered in the *yki*RNAi wing discs (Fig. 3C). These results indicate that JNK signaling may be a key mediator for *yki*-dependent ACE and BCE.

Activation of JNK signaling is necessary and sufficient to induce ACE and BCE

Our transcriptome data indicated increased expression of the JNK targets *puc* and *Matrix metalloproteinase 1* (*Mmp1*) (Fig. 3C; Martín-Blanco et al., 1998; Xue et al., 2007). To confirm activation of the JNK pathway by *yki* suppression, we examined the expression levels of a *puc-LacZ* reporter and Mmp1 protein levels. Indeed, both *puc* and Mmp1 were upregulated in *ykiRNAi* wing discs (Fig. S5). To test whether JNK signaling is required for *ykiRNAi*-induced ACE and BCE, we inhibited JNK signaling by co-expressing a dominant-negative form of JNK (bsk^{DN}) (Weber et al., 2000). Both ACE and BCE were largely blocked by bsk^{DN} in *ykiRNAi* wing discs (Fig. 4A,B). The percentage of wing discs with ACE and BCE was reduced to 10% (n=30; Fig. S3A,C). Activation of the JNK pathway by expressing hep^{CA} (a constitutively active form of *hep*), which encodes a JNK kinase (Glise et al., 1995), induced both ACE and BCE (Fig. 4C; Fig. S3B,D). To rule out the effect of apoptosis, we suppressed cell death by co-expressing *p35* with hep^{CA}. ACE and BCE were still observed (Fig. 4D) with high frequencies (55.6 and 100% for ACE and BCE, respectively; Fig. S3B,D). Taken together, these results suggest that activated JNK signaling is required and sufficient to induce ACE and BCE in the *Drosophila* wing epithelia.

Ets21c mediates ACE induced by activation of the Hpo-Yki-JNK pathway

To identify genes downstream of Yki-JNK that mediate ACE, we performed a targeted genetic screen by either overexpressing or knocking down the expression of candidate genes identified in the

Development (2020) 147, dev190124. doi:10.1242/dev.190124

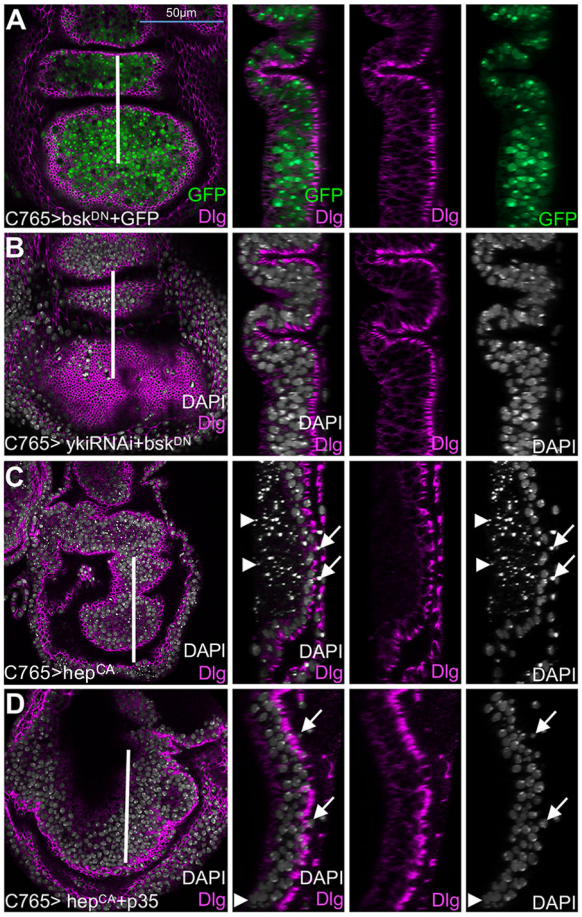

Fig. 4. JNK signaling mediates Yki-dependent ACE and BCE. (A-D) Images of wing imaginal discs are presented as described for Fig. 1. (A) Control experiment of *bsk^{DN}* expression. (B) Both ACE and BCE are prevented by co-expressing *bsk^{DN}* and *ykiRNAi*. (C) Expression of *hep^{CA}* induced ACE (arrows) and BCE (arrowheads, broken cell nuclei). (D) ACE (arrows) and BCE (arrowhead) were not prevented by co-expression of *p35* and *hep^{CA}*. White vertical lines in the *x-y* section images (left) show the location of the *y-z* images.

transcriptome analysis. We found that the Ets21c ETS-domain transcription factor, encoded by an ortholog of the proto-oncogenes *FLI1* and *ERG*, was a regulator of ACE. Similar to the results in *ykiRNAi* wing discs, expression of *Ets21c* was highly upregulated in wing discs expressing *hep^{CA}* (Fig. S6). *UAS-Ets21c^{HA}* (HA-tagged *Ets21C*) clones were eliminated from the wing disc pouch (Fig. 5A; Fig. S1G), phenocopying the *ykiRNAi* clones (Fig. S1D,G). RT-qPCR showed that *Ets21c* transcription was upregulated in *ykiRNAi* wing discs (Fig. 3D), which is consistent with our RNA-seq data (Fig. 3B). Ets21c expression was also examined using a GFP-trap line (Khan et al., 2017). Consistently, compared with the control (Fig. 5B,B′), *ykiRNAi* expression increased Ets21c-GFP levels (Fig. 5C,C′). These results suggest that Ets21c acts downstream of *yki*. The *y-z* views showed that the Ets21c-GFP level was relatively higher in cells undergoing apical extrusion (Fig. 5C,C′, yellow arrow) than that in non-extruded cells (Fig. 5C,C′). We also observed higher levels of Ets21c-GFP in apically extruding cells induced by *hep^{CA}* (Fig. S6B, yellow arrow). These results suggest that Ets21c might act downstream of *yki* and JNK to regulate ACE. To further confirm that Ets21c functions in Yki-JNK-mediated cell extrusion, *Ets21cRNAi* was co-expressed with *ykiRNAi*. Remarkably, suppressing *Ets21c* efficiently rescued the ACE but not the BCE induced by *ykiRNAi* (Fig. 5D,E, arrowheads). Co-expression of *Ets21cRNAi* with *ykiRNAi* resulted in 18.2% and 60.6% of wing discs with ACE and BCE, respectively (Fig. S3A,C; *n*=33). These results suggest that *Ets21c* upregulation mediates ACE induced by silenced *yki*. We then expressed *Ets21c^{HA}* to examine whether ACE can be induced by Ets21c. Notably, expression of *UAS-Ets21c^{HA}* was sufficient to induce ACE in 51.5% of wing discs (*n*=33) (Fig. 5F; Fig. S3B). We inspected anti-cleaved-caspase-3 staining in wing discs expressing activated *Ets21c* and did not find apparent cell death at the apical side of the epithelia (Fig. S7), which implies that there was no correlation between *Ets21c^{HA}*-induced ACE and cell apoptosis. These results further confirm that Ets21c mediates Hpo-Yki-JNK-dependent ACE.

DISCUSSION

Cell extrusion plays an important role in epithelial homeostasis and development as well as in cancer cell metastasis (Eisenhoffer et al., 2012; Gu and Rosenblatt, 2012; Gudipaty and Rosenblatt, 2017; Marinari et al., 2012; Ohsawa et al., 2018). In *Drosophila* epithelia, BCE occurs during dorsal closure and epithelial-mesenchymal transition (EMT) as well as in apoptosis (Andrade and Rosenblatt, 2011; Riesgo-Escovar et al., 1996; Riesgo-Escovar and Hafen, 1997; Pocha and Montell, 2014), whereas ACE occurs in tumor invasion and extrusion of apoptotic enterocytes in the *Drosophila* adult midgut (Dunn et al., 2018; Tamori et al., 2016; Vaughen and Igaki, 2016; Martin et al., 2018). However, the molecular mechanisms underlying BCE and ACE in *Drosophila* epithelia are not well understood. Our results demonstrate that inappropriate Hpo-Yki-JNK signaling induces ACE and BCE in *Drosophila* wing disc epithelia (Fig. 6). We also show that in the wing disc epithelia, *ban* acts downstream of Yki to regulate BCE (Fig. 6B) and *Ets21c* acts downstream of JNK to regulate ACE (Fig. 6C).

Activated Hpo pathway induces cell extrusion in the *Drosophila* wing disc epithelia

The Hpo pathway regulates tissue growth in *Drosophila* (Halder and Johnson, 2011). It has been reported that *yki^{B5}* mutant clones grow poorly in the wing and eye discs (Huang et al., 2005; Koontz et al., 2013; Qing et al., 2014). Consistent with these reports, our results showed small *ykiRNAi* and *yki^{B5}* mutant clones (Fig. 1B,D; Fig. S1B,D). Cells with depleted *yki* expression are extruded either apically or basally from the epithelia independently of apoptosis (Fig. 1F, Fig. 2D; Fig. S4C), indicating that cell extrusion is one explanation for the low recovery rate of Yki-depleted clones. In the *Drosophila* wing disc, overexpression of *hpo* by *MS1096-Gal4* and *nub-Gal4* dramatically decreases adult wing size (Koontz et al., 2013). Meanwhile, overexpression of *wts* by *nub-Gal4* also reduces the wing size (Deng et al., 2015). When we activated *hpo* and *wts* expression, using *C765-Gal4*, cells were intensively extruded to the lumen and the basal side of the epithelia (Fig. 1G,H). Therefore, in addition to the proliferation defect, cell extrusion is one reason for the reduced tissue size induced by Hpo pathway activation. Diap1 levels are decreased in the small *yki* mutant clones (Qing et al., 2014), and co-expression of *Diap1* and *ykiRNAi* could not block ACE or BCE (Fig. 2D). These results indicate that Diap1 does not regulate cell extrusion downstream of Yki. *Hpo*, *wts* mutant and *yki* overexpression in clones confers on cells supercompetitive properties that can lead to elimination of surrounding wild-type cells (Tyler et al., 2007; Ziosi et al., 2010). This suggests that cell competition could promote elimination of Yki-depleted clones. In our results, however, elimination of Yki-depleted cells could be triggered autonomously, even when Yki was depleted in the whole wing pouch. Cells expressing low levels of Myc are extruded

Development (2020) 147, dev190124. doi:10.1242/dev.190124

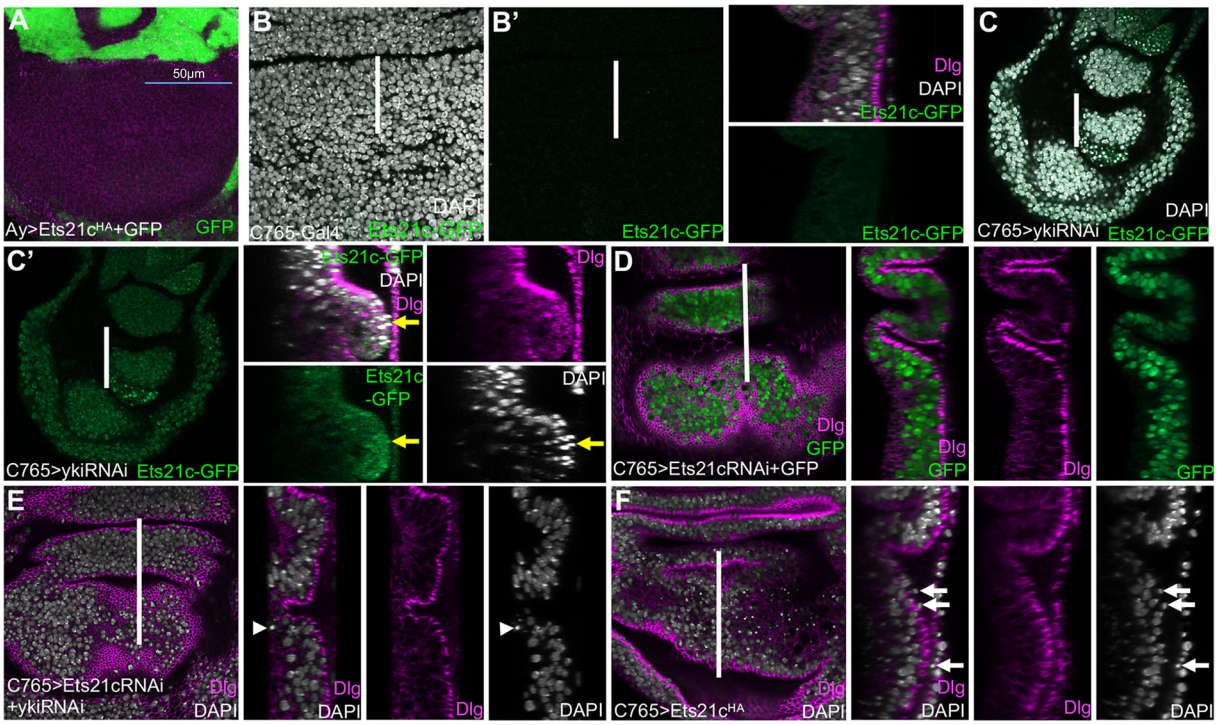

Fig. 5. Ets21c mediates JNK-dependent ACE. (A) Clones overexpressing *Ets21c*^{HA} (marked by *GFP* co-expression) are very rarely observed in the wing disc pouch. (B,B′) *Ets21c-GFP* level is low in control wing discs. (C,C′) *Ets21c-GFP* level is higher in *ykiRNAi*-expressing wing discs than in the control. The *Ets21c-GFP* level was elevated at the position of ACE (yellow arrow). (D) Expression of *Ets21cRNAi* did not induce cell extrusion. (E) Co-expression of *Ets21cRNAi* and *ykiRNAi* largely rescued ACE, but not BCE (arrowhead). (F) Expression of *Ets21c*^{HA} was sufficient to induce ACE (arrows). White vertical lines in the *x-y* section images (left) show the location of the *y-z* images.

basally through cell competition (Lampaya and Basler, 2002). Expressing *Myc* alone is not sufficient to prevent the elimination of *yki* mutant cells (Ziosi et al., 2010). Consistently, overexpression of *Myc* could not block BCE induced by silenced *yki* (Fig. 2F), indicating that other factors regulate BCE downstream of Yki. We found that *ban* could inhibit *ykiRNAi*-mediated BCE but not ACE (Fig. 2B). It is known that activated Hpo plays a role in cell migration (Ma et al., 2017). Cells with depleted *yki* expression migrated across the AP boundary and were extruded basally, and this cell migration was suppressed by *ban*. Our results show that *ban* can suppress *ykiRNAi*-induced BCE in the *Drosophila* wing disc but does not regulate *ykiRNAi*-induced ACE.

In vertebrate epithelia, cells dying through apoptosis or crowding stress are extruded apically into the lumen (Eisenhoffer et al., 2012; Rosenblatt et al., 2001; Slattum and Rosenblatt, 2014). The S1P-S1P2 pathway regulates both apoptosis-induced and apoptosis-independent ACE (Eisenhoffer et al., 2012; Gu et al., 2011; Kuipers et al., 2014). The oncogenic *KRAS*^{V12G} mutation in MDCK (Madin-Darby canine kidney) epithelial cell monolayers can downregulate both S1P (sphingosine 1-phosphate) and its receptor S1P2 (also

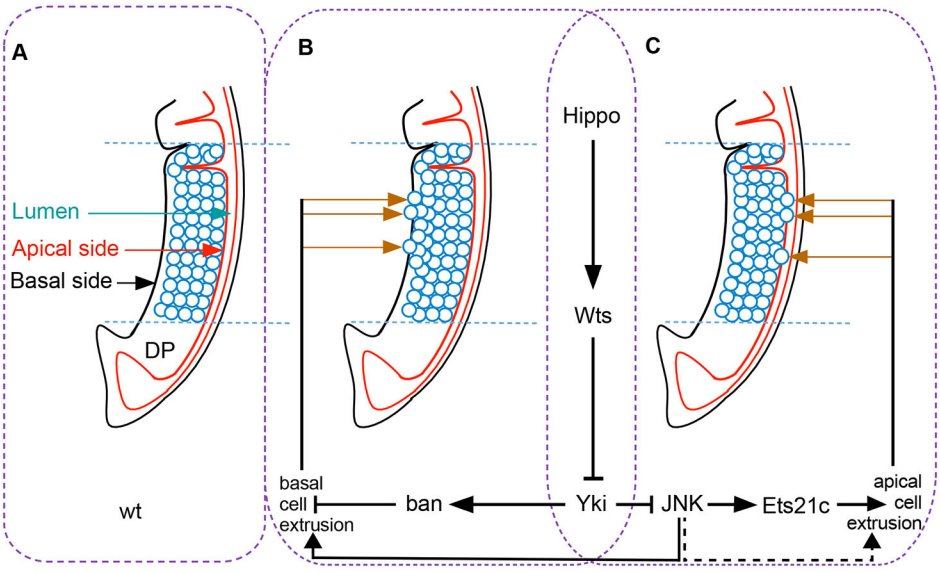

Fig. 6. A model to interpret how the Hpo pathway activates ACE and BCE. (A) In controls (wt), DP cell nuclei were observed in the middle/center of the cell layer, but never close to the basal membrane or within the overlying wing disc lumen. (B) Hpo-Yki-ban mediated BCE. (C) Ets21c mediated Hippo-JNK-dependent ACE.

Development (2020) 147, dev190124. doi:10.1242/dev.190124

known as S1PR2) to promote basal extrusion (Slattum et al., 2014). In *Drosophila* epithelia, the direction of apoptotic cell extrusion is reversed with most apoptotic cells undergoing BCE (Casas-Tintó et al., 2015; Dekanty et al., 2012). Apoptosis-induced BCE is regulated by JNK signaling (Andrade and Rosenblatt, 2011). One exception is in *Drosophila* adult midgut, where enterocytes are lost through apical extrusion (Martin et al., 2018). However, we know little about the mechanism of ACE in *Drosophila* epithelia.

In *Drosophila* epithelia, apical extrusion of *scrib* mutant cells is mediated by the Slit-Robo2-Ena complex, reduced E-cadherin and elevated Sqh levels. In normal cells, *slit*, *robo2* and *ena* overexpression only results in BCE when cell death is blocked (Vaughen and Igaki, 2016). More importantly, in our RNA-seq results, expression of *slit*, *robo2* and *ena* were not changed in the Yki-depleted *Drosophila* wing disc, which means Slit-Robo2-Ena does not associate with the Hpo pathway to regulate ACE. *scrib* mutant cells activate Jak-Stat signaling and undergo ACE in the 'tumor hotspot' located in the dorsal hinge region of the *Drosophila* wing disc (Tamori et al., 2016). Moreover, ACE can precede M6-deficient Ras^{V12} tumor invasion following elevation of Cno-RhoA-MyoII (Dunn et al., 2018). Our RNA-seq results revealed that the expression of Jak-Stat pathway genes and *RhoA* (*Rho1*) were not altered, indicating that ACE can be regulated by novel signaling pathways.

JNK signaling mediates Hpo activation-induced cell extrusion

In *Drosophila*, the JNK signaling pathway is essential for regulating cell extrusion in phenomena including wound healing, cell competition, apoptosis and dorsal closure (Ohsawa et al., 2018). JNK signaling mediates the role of Dpp and its downstream targets in cell survival regulation in the *Drosophila* wing (Adachi-Yamada et al., 1999). Cell extrusion and retraction toward the basal side of the wing epithelia induced by the lack of Dpp activity is independent of JNK (Shen and Dahmann, 2005; Shen et al., 2010). In one case of ectopic fold formation at the AP boundary of the *Drosophila* wing, loss of Omb activates both Yki and JNK signaling. In this case, JNK signaling induces the AP fold by cell shortening, and Yki signaling suppresses JNK-dependent apoptosis in the folded cells (Liu et al., 2016). During cell competition induced by Myc manipulation, JNK-dependent apoptosis mediates the death of 'loser' cells and their extrusion to the basal side of the epithelia. Apoptosis-induced BCE can be blocked by Diap1, which suppresses JNK-dependent apoptosis (Lampaya and Basler, 2002). Taken together, these results show that JNK signaling mediates or interacts with Yki signaling in a cellular context-dependent manner during the regulation of wing epithelial morphogenesis and apoptosis.

JNK is required for the migration of *Csk* mutant cells across the AP boundary and for their extrusion to the basal side of the epithelia (Vidal et al., 2006). *puc* encodes a JNK-specific phosphatase that provides feedback inhibition to specifically repress JNK activity. Expression of *puc* can prevent *ptc>CskRNAi* cells from spreading at the AP boundary (Vidal et al., 2006). JNK activity is also needed for *ykiRNAi* cells to invade across the wing disc AP boundary, and co-expression of bsk^{DN} and *ykiRNAi* blocks this invasion (Ma et al., 2017). Consistent with the role of JNK in BCE regulation, blocking JNK signaling by bsk^{DN} expression prevented *ykiRNAi* cells from being extruded to the basal side of the wing epithelia (Fig. 4B). More importantly, we found that JNK activation by hep^{CA} was sufficient to induce BCE (Fig. 4C), independently of apoptosis (Fig. 4D). Furthermore, few JNK targets have been shown to regulate cell migration and BCE. An exception to this are caspases that function downstream of JNK, which can promote cell migration when activated at a mild level (Fan et al., 2020; Rudrapatna et al., 2013).

In *Drosophila* eye imaginal discs, elevated JNK signaling in *scrib* mutant cells regulates both ACE and BCE. JNK and Robo2-Ena constitute a positive-feedback loop that promotes the apical and basal extrusion of *scrib* mutant cells through E-cadherin reduction. Meanwhile, in normal cells, p35 upregulation when *Robo2* and *Ena* are overexpressed only induces BCE (Vaughen and Igaki, 2016). Our results showed that blocking JNK signaling could suppress ACE induced by silenced *yki* (Fig. 4B). Meanwhile, activation of JNK by hep^{CA} was sufficient to induce the extrusion of cells into the lumen (Fig. 4C). Cell debris may be trapped in the disc lumen when overexpressing hep^{CA} (Herrera et al., 2013). We suppressed apoptosis by co-expressing *p35*, to confirm that the ACE observed was independent of cell death (Fig. 4D). Taken together, these results indicate that there are additional regulators downstream of JNK to mediate ACE in normal cells.

Ets21c mediates the regulation of ACE by JNK

E-twenty-six (ETS) family transcription factors have conserved functions in metazoans (Hollenhorst et al., 2011; Sharrocks et al., 1998). These include apoptosis regulation (Sevilla et al., 1999), cell differentiation promotion (Taylor et al., 1997), cell fate regulation (Miley et al., 2004) and cellular senescence (Ohtani et al., 2001). *Ets21c* encodes a member of the ETS-domain transcription factor family and is the ortholog of the human proto-oncogenes *FLI1* and *ERG* (Mundorf et al., 2019). In *Drosophila* eye imaginal discs, 30-fold increased *Ets21c* expression is induced by Ras^{V12} and *eiger*, an activator of JNK (Toggweiler et al., 2016). In the *Drosophila* adult midgut, *Ets21c* expression is increased when JNK is activated by the JNK kinase *hep* (Mundorf et al., 2019). Ets21c can also promote tumor growth downstream of the JNK pathway (Külshammer et al., 2015; Toggweiler et al., 2016). Our results have confirmed that Ets21c functions downstream of JNK. Indeed, we showed that Ets21c-GFP level was elevated following JNK activation (Fig. S6A). Expression of $Ets21c^{HA}$ was sufficient to induce ACE (Fig. 5F) and silencing of *Ets21c* was sufficient to rescue *ykiRNAi*-induced ACE in the wing discs (Fig. 5E). However, the mechanism through which *yki* regulates JNK-Ets21c remains to be determined.

In *Drosophila* imaginal discs, ACE promotes polarity-impaired cells to grow into tumors (Tamori et al., 2016; Vaughen and Igaki, 2016). Therefore, it is possible that Ets21c can promote Hpo-Yki-JNK-related tumorigenesis by facilitating ACE in *Drosophila*. It is difficult to infer a putative pro-tumoral function of Et21c in mammals through its effect on ACE. ACE is rather associated with the elimination of tumor cells in mammals (Kajita and Fujita, 2015; Kon et al., 2017), whereas BCE is traditionally associated with higher invasive capacity. Yki/YAP gain-of-function promotes cancer cell invasion in non-small-cell lung cancer (Wang et al., 2010), neoplastic transformation (Yang et al., 2013), uveal melanoma (Yu et al., 2014) and pancreatic cancer (Yang et al., 2015). Additionally, Yki/YAP loss of function helps tumor cells to escape from apoptosis in hematologic malignancies, including multiple myeloma, lymphoma and leukemia (Cottini et al., 2014). Consistent with the latter role, Yki suppressed cell extrusion from the *Drosophila* wing epithelia by suppressing Ets21c (Fig. 5E). Therefore, the role of Ets21c in Hpo-Yki-related tumor models should be further examined.

MATERIALS AND METHODS

Drosophila genetics

The following transgenes were used in this study: *C765-Gal4* (Nellen et al., 1996), *UAS-*bsk^{DN} (Weber et al., 2000), *UAS-ban* (Ying and Padgett, 2012),

Development (2020) 147, dev190124. doi:10.1242/dev.190124

puc-lacZ (Martín-Blanco et al., 1998), *FRT42D-yki^{B5}* and *FRT42D* (gifts from Z. H. Li, Capital Normal University, Beijing, China), *UAS-Diap1* (gift from A. Bergmann, University of Massachusetts Medical School, Worcester, MA, USA), *UAS-hippo* and *UAS-wts* (gifts from L. Xue, Tongji University, Shanghai, China), *UAS-GFP* [Bloomington Drosophila Stock Center (BL), #4775], *UAS-CycE* (BL, #30725), *UAS-Myc* (BL, #9674), *UAS-p35* (BL, #5073), *UAS-hep^{CA}* (BL, #38639), *Ets21c-GFP* (BL, #38639), *UAS-Ets21cRNAi* (Vienna *Drosophila* Resource Center, #106153), *UAS-Ets21c^{HA}* (FlyORF, #F000624), *UAS-ykiRNAi* [Tsinghua University (THU), #0579] and *UAS-ykiRNAi* (THU, #3074).

Transgene expression and clonal induction

Larvae were raised at 25°C. For efficient expression of *RNAi* and *UAS* transgenes driven by *C765-Gal4*, larvae were raised at 29°C. To generate *UAS-ykiRNAi* and *UAS-Ets21c* clones, larvae of genotype *y w hs-Flp*/+; *act5c>CD2>Gal4*, *UAS-GFP*/+; *UAS-ykiRNAi*/+ and *y w hs-Flp*/+; *act5c>CD2>Gal4*, *UAS-GFP*/+; *UAS-Ets21c*/+ were subjected to heat shock at 35°C for 30 min. To generate *yki^{B5}* MARCM clones, larvae of genotype *y w hs-flp*, *tub-Gal4*, *UAS-GFP*/+; *FRT42D*, *Tub-Gal80*/*FRT42D yki^{B5}* were subjected to heat shock for 1 h at 37.5°C. Larval genotypes for the data shown in every figure are listed in Table S5.

Immunohistochemistry

Drosophila wing imaginal discs were dissected from middle to late third instar larvae, and antibody staining was performed according to standard procedures (Sui et al., 2012). The primary antibodies used were: mouse anti-Dlg1 (1:10; 4F3; Developmental Studies Hybridoma Bank, DSHB); rabbit anti-cleaved caspase-3 (1:200; Asp175; Cell Signaling); mouse anti-Mmp1 (1:10; 5H7B11; DSHB); and mouse anti-β-galactosidase, (1:2000; Z3783; Promega). Secondary antibodies (diluted 1:200) used were anti-mouse Cy3, anti-rabbit Cy3 and anti-rat Cy3 (Jackson Immuno Research). The cell membrane was stained using rhodamine-phalloidin (1:1000; PHDR1; Sigma). Cell nuclei were stained with DAPI (1:200,000; 32670; Sigma).

Images collection and analysis

Images were collected using Leica SP8 and Zeiss LSM 800 confocal microscopes. The figures were assembled in Adobe Photoshop CC with minor image adjustments (brightness and/or contrast). To compare the Ets21c-GFP fluorescence intensity in Fig. 5 and Fig. S6, staining and microscopy conditions were identical, and images were edited in parallel using Adobe Photoshop CC.

Cell extrusion criteria

More than ten *Drosophila* wing pouches were *y-z* scanned to statistically assay BCE and ACE. In controls, DP cell nuclei were observed in the middle/center of the cell layer, but never close to the basal membrane or within the overlying wing disc lumen. The BCE and ACE were defined as the presence of a cell nucleus close to the basal membrane and within the overlying wing disc lumen, respectively, especially when the cell nucleus was located outside of the basal membrane or in the lumen (Fig. 6).

RNA-seq

C765>ykiRNAi wing discs were dissected as test samples, and *C765>* wing discs were dissected as controls. For each sample, 100 wing discs were dissected in PBS on ice. Total RNA was prepared using Trizol reagent (Invitrogen, code no. 12183555) following the recommendations of the manufacturer. RNA quality was verified by agarose gel electrophoresis and using a Nanodrop 2000. RNA-seq libraries were sequenced on an Illumina Hiseq platform. Raw reads were processed to clean data using in-house Perl scripts. Clean data were mapped to the *Drosophila* genome using TopHat v2.0.12 (Kim et al., 2013). Analysis of differential expression in test and control samples was performed using the DESeq2 R package (Anders and Huber, 2010). Genes with DESeq2 adjusted *P*-values<0.01 were considered to be differentially expressed. KOBAS software (http://kobas.cbi.pku.edu.cn/kobas3/?t=1) was used to test the statistical enrichment of differentially expressed genes in KEGG pathways (http://www.genome.jp/kegg/). We also used DAVID to test the GO functional enrichment of differentially expressed genes (https://david.ncifcrf.gov).

RT-qPCR

cDNA was reversed transcribed from RNA using the TaKaRa PrimeScript RT reagent kit with gDNA Eraser (code no. RR047A). RT-qPCR was performed using the PerfectStart Green qPCR SuperMix (+Dye II) (TransGen Biotech) in the QuantStudio 6 Flex platform (Applied Biosystems), and each reaction was repeated in triplicate. Transcription levels were normalized to those of *act*. Data were calculated using Microsoft Excel and presented as mean+s.d. *P* values were calculated using two-tailed Student's *t*-test: **P*<0.05; ***P*<0.01; ****P*<0.001. The gene-specific primer sequences used are shown in Table S4.

Statistical analysis

For quantifying the number of clones in the pouch, between eight and ten third instar transgenic larvae were selected at random from three groups, images were taken at 0.5 µm increments along the *z*-axis using a Leica SP8 confocal microscope. Image stacks were used to quantify the number of separate clones in the pouch. Clone numbers were analyzed using GraphPad Prism 7. For quantification of the percentage of ACE and BCE, transgenic flies were raised as previously described in 'Transgene expression and clonal induction', three groups (each group having more than 25 larvae) of third instar wing discs were dissected and scored for the percentage of ACE and BCE. The experimental data were calculated using Microsoft Excel and presented as mean+s.d. *P* values were calculated using two-tailed Student's *t*-test. **P*<0.05; ***P*<0.01; ****P*<0.001; *****P*<0.0001; n.s., no significant difference.

Acknowledgements

We thank Dr L. Xue, Dr Z. H. Li, Dr A. Bergmann, Bloomington Stock Center, Vienna *Drosophila* RNAi Center and Tsinghua University Stock Center for fly stocks, and Dr N. Jiang and Dr L. Qi for the confocal facilities.

Competing interests

The authors declare no competing or financial interests.

Author contributions

Conceptualization: D.W., J.S.; Investigation: X.A.; Writing - original draft: X.A., D.W., J.S.; Writing - review & editing: D.W., J.Z., J.S.; Supervision: J.S.; Project administration: J.S.; Funding acquisition: D.W., J.S.

Funding

This research was financially supported by the National Natural Science Foundation of China (NSFC32030012, NSFC31872295 and NSFC31872293).

Data availability

RNA-seq data has been deposited in NCBI under accession number PRJNA678029.

Supplementary information

Supplementary information available online at https://dev.biologists.org/lookup/doi/10.1242/dev.190124.supplemental

Peer review history

The peer review history is available online at https://dev.biologists.org/lookup/doi/10.1242/dev.190124.reviewer-comments.pdf

References

Adachi-Yamada, T., Fujimura-Kamada, K., Nishida, Y. and Matsumoto, K. (1999). Distortion of proximodistal information causes JNK-dependent apoptosis *Drosophila* wing. *Nature* **400**, 166-169. doi:10.1038/22112

Anders, S. and Huber, W. (2010). Differential expression analysis for sequence count data. *Genome Biol.* **11**, R106. doi:10.1186/gb-2010-11-10-r106

Andrade, D. and Rosenblatt, J. (2011). Apoptotic regulation of epithelial cellular extrusion. *Apoptosis* **16**, 491-501. doi:10.1007/s10495-011-0587-z

Atkins, M., Potier, D., Romanelli, L., Jacobs, J., Mach, J., Hamaratoglu, F., Aerts, S. and Halder, G. (2016). An ectopic network of transcription factors regulated by hippo signaling drives growth and invasion of a malignant tumor model. *Curr. Biol.* **26**, 2101-2113. doi:10.1016/j.cub.2016.06.035

Casas-Tintó, S., Lolo, F.-N. and Moreno, E. (2015). Active JNK-dependent secretion of *Drosophila* Tyrosyl-tRNA synthetase by loser cells recruits haemocytes during cell competition. *Nat. Commun.* **6**, 10022. doi:10.1038/ncomms10022

Cottini, F., Hideshima, T., Xu, C., Sattler, M., Dori, M., Agnelli, L., Hacken, E. t., Bertilaccio, M. T., Antonini, E., Neri, A. et al. (2014). Rescue of Hippo

coactivator YAP1 triggers DNA damage-induced apoptosis in hematological cancers. *Nat. Med.* **20**, 599-606. doi:10.1038/nm.3562

Dekanty, A., Barrio, L., Muzzopappa, M., Auer, H. and Milán, M. (2012). Aneuploidy-induced delaminating cells drive tumorigenesis in *Drosophila* epithelia. *Proc. Natl. Acad. Sci. USA* **109**, 20549-20554. doi:10.1073/pnas.1206675109

Deng, H., Wang, W., Yu, J., Zheng, Y., Yun, Q. and Pan, D. (2015). Spectrin regulates Hippo signaling by modulating cortical actomyosin activity. *elife* **4**, e06567. doi:10.7554/eLife.06567

Dong, J., Feldmann, G., Huang, J., Wu, S., Zhang, N., Comerford, S. A., Gayyed, M. F., Anders, R. A., Maitra, A. and Pan, D. (2007). Elucidation of a universal size-control mechanism in *Drosophila* and mammals. *Cell* **130**, 1120-1133. doi:10.1016/j.cell.2007.07.019

Dunn, B. S., Rush, L., Lu, J.-Y. and Xu, T. (2018). Mutations in the *Drosophila* tricellular junction protein M6 synergize with Ras^{V12} to induce apical cell delamination and invasion. *Proc. Natl. Acad. Sci. USA* **115**, 8358-8363. doi:10.1073/pnas.1807343115

Eisenhoffer, G. T., Loftus, P. D., Yoshigi, M., Otsuna, H., Chien, C.-B., Morcos, P. A. and Rosenblatt, J. (2012). Crowding induces live cell extrusion to maintain homeostatic cell numbers in epithelia. *Nature* **484**, 546-549. doi:10.1038/nature10999

Fan, W., Luo, D., Zhang, J., Wang, D. and Shen, J. (2020). Vestigial suppresses apoptosis and cell migration in a manner dependent on the level of JNK/Caspase signaling in the *Drosophila* wing disc. *Insect Sci.* [Epub] doi:10.1111/1744-7917.12762

Feng, X., Degese, M. S., Iglesias-Bartolome, R., Vaque, J. P., Molinolo, A. A., Rodrigues, M., Zaidi, M. R., Ksander, B. R., Merlino, G., Sodhi, A. et al. (2014). Hippo-independent activation of YAP by the GNAQ uveal melanoma oncogene through a trio-regulated rho GTPase signaling circuitry. *Cancer Cell* **25**, 831-845. doi:10.1016/j.ccr.2014.04.016

Glise, B., Bourbon, H. G. and Noselli, S. (1995). hemipterous encodes a novel *Drosophila* MAP kinase kinase, required for epithelial cell sheet movement. *Cell* **83**, 451-461. doi:10.1016/0092-8674(95)90123-X

Gu, Y. and Rosenblatt, J. (2012). New emerging roles for epithelial cell extrusion. *Curr. Opin. Cell Biol.* **24**, 865-870. doi:10.1016/j.ceb.2012.09.003

Gu, Y., Forostyan, T., Sabbadini, R. A. and Rosenblatt, J. (2011). Epithelial cell extrusion requires the sphingosine-1-phosphate receptor 2 pathway. *J. Cell Biol.* **193**, 667-676. doi:10.1083/jcb.201010075

Gudipaty, S. A. and Rosenblatt, J. (2017). Epithelial cell extrusion: pathways and pathologies. *Semin. Cell Dev. Biol.* **67**, 132-140. doi:10.1016/j.semcdb.2016.05.010

Halder, G. and Johnson, R. L. (2011). Hippo signaling: growth control and beyond. *Development* **138**, 9-22. doi:10.1242/dev.045500

Harrison, D. A. and Perrimon, N. (1993). Simple and efficient generation of marked clones in *Drosophila*. *Curr. Biol.* **3**, 424-433. doi:10.1016/0960-9822(93)90349-S

Hay, B. A., Wassarman, D. A. and Rubin, G. M. (1995). *Drosophila* homologs of baculovirus inhibitor of apoptosis proteins function to block cell death. *Cell* **83**, 1253-1262. doi:10.1016/0092-8674(95)90150-7

Herrera, S. C., Martín, R. and Morata, G. (2013). Tissue homeostasis in the wing disc of *Drosophila melanogaster*: immediate response to massive damage during development. *PLoS Genet.* **9**, e1003446. doi:10.1371/journal.pgen.1003446

Hollenhorst, P. C., McIntosh, L. P. and Graves, B. J. (2011). Genomic and biochemical insights into the specificity of ETS transcription factors. *Annu. Rev. Biochem.* **80**, 437-471. doi:10.1146/annurev.biochem.79.081507.103945

Huang, J., Wu, S., Barrera, J., Matthews, K. and Pan, D. (2005). The Hippo signaling pathway coordinately regulates cell proliferation and apoptosis by inactivating Yorkie, the *Drosophila* Homolog of YAP. *Cell* **122**, 421-434. doi:10.1016/j.cell.2005.06.007

Kajita, M. and Fujita, Y. (2015). EDAC: epithelial defence against cancer—cell competition between normal and transformed epithelial cells in mammals. *J. Biochem.* **158**, 15-23. doi:10.1093/jb/mvv050

Khan, S. J., Abidi, S. N. F., Skinner, A., Tian, Y. and Smith-Bolton, R. K. (2017). The *Drosophila* Duox maturation factor is a key component of a positive feedback loop that sustains regeneration signaling. *PLoS Genet.* **13**, e1006937. doi:10.1371/journal.pgen.1006937

Kim, D., Pertea, G., Trapnell, C., Pimentel, H., Kelley, R. and Salzberg, S. L. (2013). TopHat2: accurate alignment of transcriptomes in the presence of insertions, deletions and gene fusions. *Genome Biol.* **14**, R36. doi:10.1186/gb-2013-14-4-r36

Kim, M., Kim, T., Johnson, R. L. and Lim, D.-S. (2015). Transcriptional Co-repressor function of the hippo pathway transducers YAP and TAZ. *Cell Reports* **11**, 270-282. doi:10.1016/j.celrep.2015.03.015

Knust, E. and Bossinger, O. (2002). Composition and formation of intercellular junctions in epithelial cells. *Science* **298**, 1955-1959. doi:10.1126/science.1072161

Kon, S., Ishibashi, K., Katoh, H., Kitamoto, S., Shirai, T., Tanaka, S., Kajita, M., Ishikawa, S., Yamauchi, H., Yako, Y. et al. (2017). Cell competition with normal epithelial cells promotes apical extrusion of transformed cells through metabolic changes. *Nat. Cell Biol.* **19**, 530-541. doi:10.1038/ncb3509

Koontz, L. M., Liu-Chittenden, Y., Yin, F., Zheng, Y., Yu, J., Huang, B., Chen, Q., Wu, S. and Pan, D. (2013). The Hippo effector Yorkie controls normal tissue growth by antagonizing scalloped-mediated default repression. *Dev. Cell* **25**, 388-401. doi:10.1016/j.devcel.2013.04.021

Kuipers, D., Mehonic, A., Kajita, M., Peter, L., Fujita, Y., Duke, T., Charras, G. and Gale, J. E. (2014). Epithelial repair is a two-stage process driven first by dying cells and then by their neighbours. *J.Cell Sci.* **127**, 1229-1241. doi:10.1242/jcs.138289

Külshammer, E., Mundorf, J., Kilinc, M., Frommolt, P., Wagle, P. and Uhlirova, M. (2015). Interplay among *Drosophila* transcription factors Ets21c, Fos and Ftz-F1 drives JNK-mediated tumor malignancy. *Dis. Models Mech.* **8**, 1279-1293. doi:10.1242/dmm.020719

Lampaya, M. E. and Basler, K. (2002). dMyc Transforms cells into super-competitors. *Cell* **117**, 117-129. doi:10.1016/S0092-8674(04)00262-4

Lee, T. and Luo, L. (2001). Mosaic analysis with a repressible cell marker (MARCM) for *Drosophila* neural development. *Trends Neurosci.* **24**, 251-254. doi:10.1016/S0166-2236(00)01791-4

Liu, S., Sun, J., Wang, D., Pflugfelder, G. O. and Shen, J. (2016). Fold formation at the compartment boundary of *Drosophila* wing requires Yki signaling to suppress JNK dependent apoptosis. *Sci. Rep.* **6**, 38003. doi:10.1038/srep38003

Ma, X., Wang, H., Ji, J., Xu, W., Sun, Y., Li, W., Zhang, X., Chen, J. and Xue, L. (2017). Hippo signaling promotes JNK-dependent cell migration. *Proc. Natl. Acad. Sci. USA* **114**, 1934-1939. doi:10.1073/pnas.1621359114

Marinari, E., Mehonic, A., Curran, S., Gale, J., Duke, T. and Baum, B. (2012). Live-cell delamination counterbalances epithelial growth to limit tissue overcrowding. *Nature* **484**, 542-545. doi:10.1038/nature10984

Martin, J. L., Sanders, E. N., Moreno-Roman, P., Jaramillo Koyama, L. A., Balachandra, S., Du, X. and O'Brien, L. E. (2018). Long-term live imaging of the *Drosophila* adult midgut reveals real-time dynamics of division, differentiation and loss. *eLife* **7**, e36248. doi:10.7554/eLife.36248

Martín-Blanco, E., Gampel, A., Ring, J., Virdee, K., Kirov, N., Tolkovsky, A. M. and Martinez-Arias, A. (1998). puckered encodes a phosphatase that mediates a feedback loop regulating JNK activity during dorsal closure in *Drosophila*. *Genes Dev.* **12**, 557-570. doi:10.1101/gad.12.4.557

Miley, G. R., Fantz, D. A., Glossip, D., Lu, X., Saito, R. M., Palmer, R. E., Inoue, T., van den Heuvel, S., Sternberg, P. W. and Kornfeld, K. (2004). Identification of residues of the caenorhabditis elegans LIN-1 ETS domain that are necessary for DNA binding and regulation of Vulval cell fates. *Genetics* **167**, 1697-1709. doi:10.1534/genetics.104.029017

Mundorf, J., Donohoe, C. D., McClure, C. D., Southall, T. D. and Uhlirova, M. (2019). Ets21c governs tissue renewal, stress tolerance, and aging in the *Drosophila* intestine. *Cell Rep.* **27**, 3019-3033. doi:10.1016/j.celrep.2019.05.025

Nellen, D., Burke, R., Struhl, G. and Basler, K. (1996). Direct and long-range action of a DPP morphogen gradient. *Cell* **85**, 357-368. doi:10.1016/S0092-8674(00)81114-9

Neto-Silva, R. M., Beco, S. D. and Johnston, L. A. (2010). Evidence for a growth-stabilizing regulatory feedback mechanism between Myc and Yorkie, the *Drosophila* homolog of yap. *Dev. Cell* **19**, 507-520. doi:10.1016/j.devcel.2010.09.009

Nolo, R., Morrison, C. M., Tao, C., Zhang, X. and Halder, G. (2006). The bantam MicroRNA is a target of the hippo tumor-suppressor pathway. *Curr. Biol.* **16**, 1895-1904. doi:10.1016/j.cub.2006.08.057

Ohsawa, S., Vaughen, J. and Igaki, T. (2018). Cell extrusion: a stress-responsive force for good or evil in epithelial homeostasis. *Dev. Cell* **44**, 284-296. doi:10.1016/j.devcel.2018.01.009

Ohtani, N., Zebedee, Z., Huot, T. J. G., Stinson, J. A., Sugimoto, M., Ohashi, Y., Sharrocks, A. D., Peters, G. and Hara, E. (2001). Opposing effects of Ets and Id proteins on p16INK4a expression during cellular senescence. *Nature* **409**, 1067-1070. doi:10.1038/35059131

Pagliarini, R. A. and Xu, T. (2003). A genetic screen in *Drosophila* for metastatic behavior. *Science* **302**, 1227-1231. doi:10.1126/science.1088474

Pan, D. (2010). The hippo signaling pathway in development and cancer. *Dev. Cell* **19**, 491-505. doi:10.1016/j.devcel.2010.09.011

Pocha, S. M. and Montell, D. J. (2014). Cellular and molecular mechanisms of single and collective cell migrations in *Drosophila*: themes and variations. *Annu. Rev. Genet.* **48**, 295-318. doi:10.1146/annurev-genet-120213-092218

Praskova, M., Xia, F. and Avruch, J. (2008). MOBKL1A/MOBKL1B phosphorylation by MST1 and MST2 inhibits cell proliferation. *Curr. Biol.* **18**, 311-321. doi:10.1016/j.cub.2008.02.006

Qing, Y., Yin, F., Wang, W., Zheng, Y., Guo, P., Schozer, F., Deng, H. and Pan, D. (2014). The Hippo effector Yorkie activates transcription by interacting with a histone methyltransferase complex through Ncoa6. *Elife* **3**, e02564. doi:10.7554/eLife.02564

Riesgo-Escovar, J. R. and Hafen, E. (1997). *Drosophila* Jun kinase regulates expression of decapentaplegic via the ETS-domain protein Aop and the AP-1 transcription factor DJun during dorsal closure. *Genes Dev.* 11, 1717-1727.

Riesgo-Escovar, J. R., Jenni, M., Fritz, A. and Hafen, E. (1996). The *Drosophila* Jun-N-terminal kinase is required for cell morphogenesis but not for DJun-dependent cell fate specification in the eye. *Genes Dev.* **10**, 2759-2768. doi:10.1101/gad.10.21.2759

Rosenblatt, J., Raff, M. C. and Cramer, L. P. (2001). An epithelial cell destined for apoptosis signals its neighbors to extrude it by an actin- and myosin-dependent mechanism. *Curr. Biol.* **11**, 1847-1857. doi:10.1016/S0960-9822(01)00587-5

Rudrapatna, V. A., Bangi, E. and Cagan, R. L. (2013). Caspase signalling in the absence of apoptosis drives Jnk-dependent invasion. *EMBO Rep.* **14**, 172-177. doi:10.1038/embor.2012.217

Schroeder, M. C. and Halder, G. (2012). Regulation of the Hippo pathway by cell architecture and mechanical signals. *Semin. Cell Dev. Biol.* **23**, 803-811. doi:10.1016/j.semcdb.2012.06.001

Sevilla, L., Aperlo, C., Dulic, V., Chambard, J. C., Boutonnet, C., Pasquier, O., Pognonec, P. and Boulukos, K. E. (1999). The Ets2 transcription factor inhibits apoptosis induced by colony-stimulating factor 1 deprivation of macrophages through a Bcl-xL-dependent mechanism. *Mol. Cell. Biol.* **19**, 2624-2634. doi:10.1128/MCB.19.4.2624

Sharrocks, A. D., Brown, A. L., Ling, Y. and Yates, P. R. (1998). The ETS-domain transcription factor family. *Int. J. Biochem. Cell Biol.* **29**, 1371-1387. doi:10.1016/S1357-2725(97)00086-1

Shen, J. and Dahmann, C. (2005). Extrusion of cells with inappropriate Dpp signaling from *Drosophila* wing disc epithelia. *Science* **307**, 1789-1790. doi:10.1126/science.1104784

Shen, J., Dahmann, C. and Pflugfelder, G. O. (2010). Spatial discontinuity of Optomotor-blind expression in the *Drosophila* wing imaginal disc disrupts epithelial architecture and promotes cell sorting. *BMC Dev. Biol.* **10**, 23. doi:10.1186/1471-213X-10-23

Shen, J., Lu, J., Sui, L., Wang, D., Yin, M., Hoffmann, I., Legler, A. and Pflugfelder, G. O. (2014). The orthologous Tbx transcription factors Omb and TBX2 induce epithelial cell migration and extrusion in vivo without involvement of matrix metalloproteinases. *Oncotarget* **5**, 11998-12015. doi:10.18632/oncotarget.2426

Slattum, G. M. and Rosenblatt, J. (2014). Tumour cell invasion: an emerging role for basal epithelial cell extrusion. *Nat. Rev. Cancer* **14**, 495-501. doi:10.1038/nrc3767

Slattum, G., Gu, Y., Sabbadini, R. and Rosenblatt, J. (2014). Autophagy in oncogenic K-Ras promotes basal extrusion of epithelial cells by degrading S1P. *Curr. Biol.* **24**, 19-28. doi:10.1016/j.cub.2013.11.029

Sui, L., Pflugfelder, G. O. and Shen, J. (2012). The Dorsocross T-box transcription factors promote tissue morphogenesis in the Drosophila wing imaginal disc. *Development* **139**, 2773-2782. doi:10.1242/dev.079384

Tamori, Y., Suzuki, E. and Deng, W.-M. (2016). Epithelial tumors originate in tumor hotspots, a tissue-intrinsic microenvironment. *PLoS Biol.* **14**, e1002537. doi:10.1371/journal.pbio.1002537

Tapon, N., Harvey, K. F., Bell, D. W., Wahrer, D. C. R., Schiripo, T. A., Haber, D. A. and Hariharan, I. K. (2002). salvador promotes both cell cycle exit and apoptosis in *Drosophila* and is mutated in human cancer cell lines. *Cell* **110**, 467-478. doi:10.1016/S0092-8674(02)00824-3

Taylor, J. M., Dupont-Versteegden, E. E., Davies, J. D., Hassell, J. A., Houlé, J. D., Gurley, C. M. and Peterson, C. A. (1997). A role for the ETS domain transcription factor PEA3 in myogenic differentiation. *Mol. Cell. Biol.* **17**, 5550-5558. doi:10.1128/MCB.17.9.5550

Thompson, B. J. and Cohen, S. M. (2006). The Hippo pathway regulates the bantam microRNA to control cell proliferation and apoptosis in *Drosophila*. *Cell* **126**, 767-774. doi:10.1016/j.cell.2006.07.013

Toggweiler, J., Willecke, M. and Basler, K. (2016). The transcription factor Ets21C drives tumor growth by cooperating with AP-1. *Sci. Rep.* **6**, 34725. doi:10.1038/srep34725

Tyler, D., Li, W., Zhuo, N., Pellock, B. and Baker, N. (2007). Genes affecting cell competition in *Drosophila*. *Genetics* **175**, 643-657. doi:10.1534/genetics.106.061929

Udan, R. S., Kango-Singh, M., Nolo, R., Tao, C. and Halder, G. (2003). Hippo promotes proliferation arrest and apoptosis in the Salvador/Warts pathway. *Nat. Cell Biol.* **5**, 914-920. doi:10.1038/ncb1050

Vaughen, J. and Igaki, T. (2016). Slit-robo repulsive signaling extrudes tumorigenic cells from epithelia. *Dev. Cell* **39**, 683-695. doi:10.1016/j.devcel.2016.11.015

Vidal, M., Larson, D. E. and Cagan, R. L. (2006). Csk-deficient boundary cells are eliminated from normal *Drosophila* epithelia by exclusion, migration, and apoptosis. *Dev. Cell* **10**, 33-44. doi:10.1016/j.devcel.2005.11.007

Wang, Y., Dong, Q., Zhang, Q., Li, Z., Wang, E. and Qiu, X. (2010). Overexpression of yes-associated protein contributes to progression and poor prognosis of non-small-cell lung cancer. *Cancer Sci.* **101**, 1279-1285. doi:10.1111/j.1349-7006.2010.01511.x

Weber, U., Paricio, N. and Mlodzik, M. (2000). Jun mediates Frizzled-induced R3/R4 cell fate distinction and planar polarity determination in the *Drosophila* eye. *Development* **127**, 3619-3629.

Wu, S., Huang, J., Dong, J. and Pan, D. (2003). hippo Encodes a Ste-20 family protein kinase that restricts cell proliferation and promotes apoptosis in conjunction with salvador and warts. *Cell* **114**, 445-456. doi:10.1016/S0092-8674(03)00549-X

Xue, L., Igaki, T., Kuranaga, E., Kanda, H., Miura, M. and Xu, T. (2007). Tumor suppressor CYLD regulates JNK-induced cell death in *Drosophila*. *Dev. Cell* **13**, 446-454. doi:10.1016/j.devcel.2007.07.012

Yang, S., Zhang, L., Liu, M., Chong, R., Ding, S.-J., Chen, Y. and Dong, J. (2013). CDK1 phosphorylation of YAP promotes mitotic defects and cell motility and is essential for neoplastic transformation. *Cancer Res.* **73**, 6722-6733. doi:10.1158/0008-5472.CAN-13-2049

Yang, S., Zhang, L., Purohit, V., Shukla, S. K., Chen, X., Yu, F., Fu, K., Chen, Y., Solheim, J., Singh, P. K. et al. (2015). Active YAP promotes pancreatic cancer cell motility, invasion and tumorigenesis in a mitotic phosphorylation-dependent manner through LPAR3. *Oncotarget* **6**, 36019-36031. doi:10.18632/oncotarget.5935

Ying, L. and Padgett, R. W. (2012). Bantam is required for optic lobe development and glial cell proliferation. *PLoS ONE* **7**, e32910. doi:10.1371/journal.pone.0032910

Yu, F.-X., Luo, J., Mo, J.-S., Liu, G., Kim, Y. C., Meng, Z., Zhao, L., Peyman, G., Ouyang, H., Jiang, W. et al. (2014). Mutant Gq/11 promote uveal melanoma tumorigenesis by activating YAP. *Cancer Cell* **25**, 822-830. doi:10.1016/j.ccr.2014.04.017

Zhang, L., Ren, F., Zhang, Q., Chen, Y., Wang, B. and Jiang, J. (2008). The TEAD/TEF family of transcription factor scalloped mediates hippo signaling in organ size control. *Dev. Cell* **14**, 377-387. doi:10.1016/j.devcel.2008.01.006

Ziosi, M., Baena-López, L. A., Grifoni, D., Froldi, F., Pession, A., Garoia, F., Trotta, V., Bellosta, P., Cavicchi, S. and Pession, A. (2010). dMyc Functions downstream of yorkie to promote the supercompetitive behavior of hippo pathway mutant cells. *PLoS Genet.* **6**, e1001140. doi:10.1371/journal.pgen.1001140

Supplementary materials

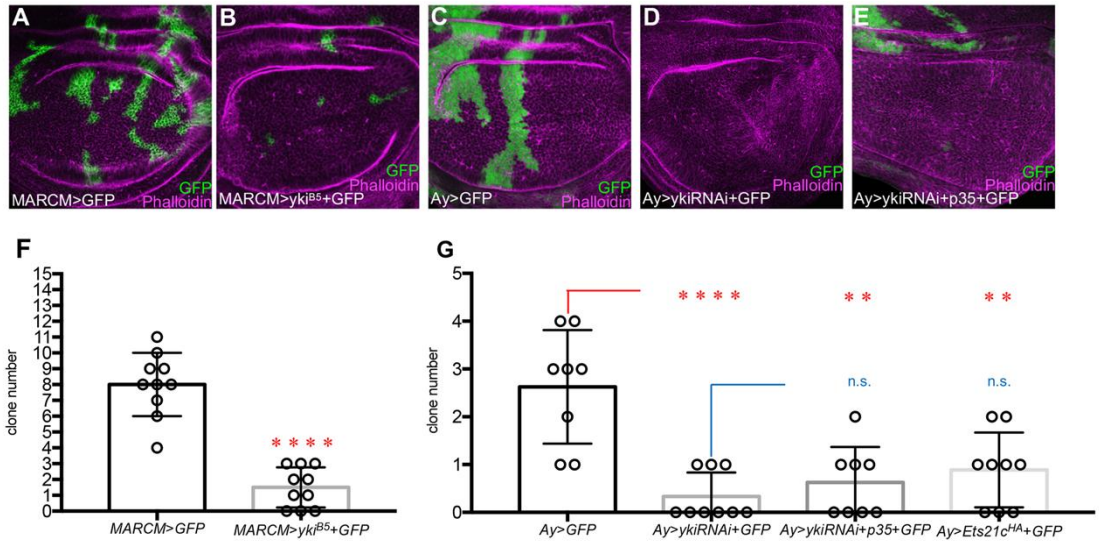

Figure S1. Lack of *yki* induced small and rare clones in the wing discs

(A) *GFP*-marked MARCM control clones in the *Drosophila* wing disc (n=). (B) *yki*^{B5} mutant clones were small and rare (n=). (C) *GFP* expressing clones (n=). (D) *ykiRNAi* clones were very rarely observed in the wing disc pouch (n=). (E) *ykiRNAi* and *p35* co-expressing clones were still rare and small (n=). (F and G) Quantification of clone numbers in A–E and Fig 5A. Data are presented as mean + SD. P values were calculated using two-tailed Student's t tests. **p < 0.01;; ****p < 0.0001; n.s., no significant difference.

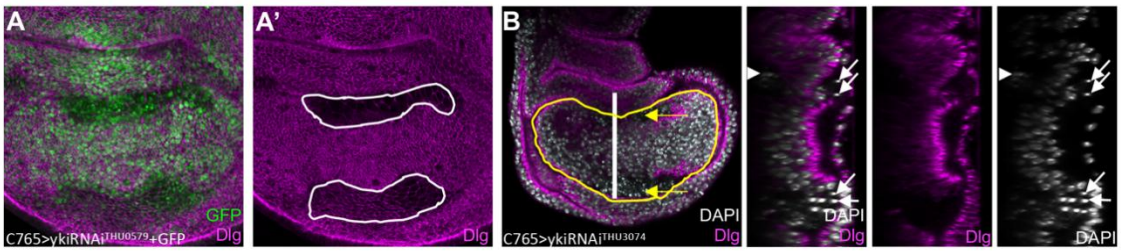

Figure S2. Apical extrusion of cells occurred intensively in two stripe regions close to the wing hinge

(A and A') x-y views close to the apical section of the wing disc showed two stripe regions with reduced Dlg staining. (B) Knocking-down *yki* in another independent *ykiRNAi* line (*UAS-ykiRNAi*^{THU3074}) induced the same apical cell extrusion (arrows) and basal cell extrusion (arrowhead) phenotypes in the wing epithelia. ACE occurred (arrows) in the pouch of the wing disc (yellow circle). *UAS-ykiRNAi*^{THU0579} and *UAS-ykiRNAi*^{THU3074} were constructed using two different vectors: VALIUM20 and VALIUM10. Furthermore, the RNAi target sequences in these two lines differ.

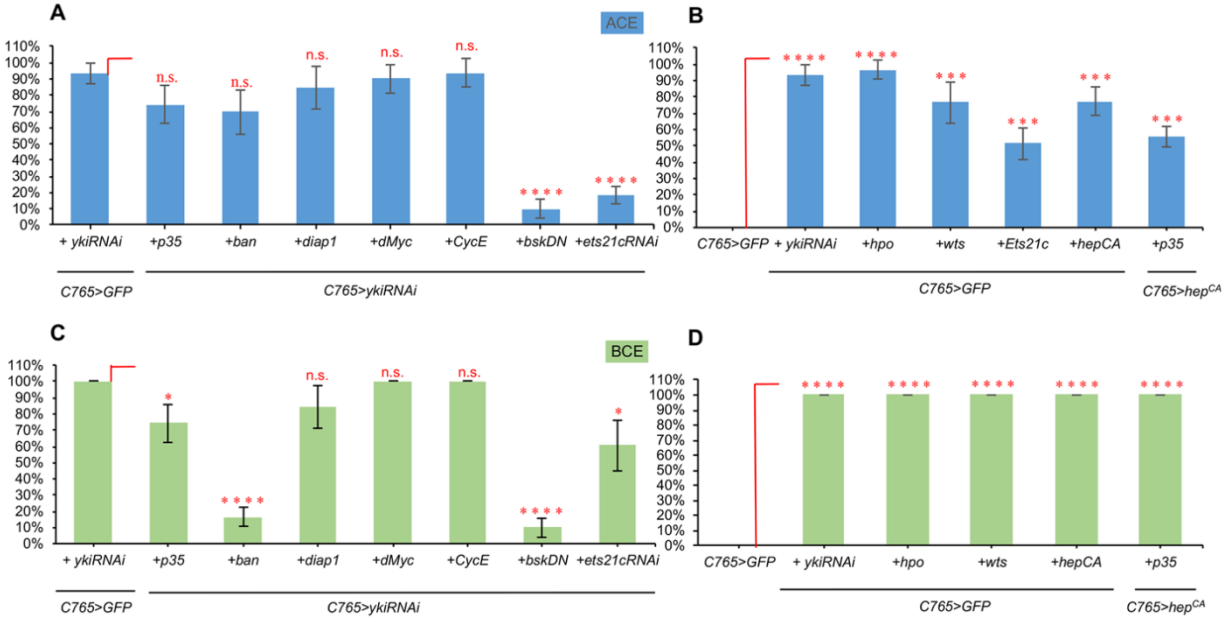

Figure S3. The percentage of wing discs with ACE and BCE

We used C765-Gal4 to drive gene expression. (A) Percentage of wing discs with ACE: *ykiRNAi+GFP* (93.3%, n=30) (n refer to average wing disc number of three replications), *ykiRNAi+p35* (74.2%, n=31), *ykiRNAi+ban* (70%, n=30), *ykiRNAi+diap1* (84.4%, n=32), *ykiRNAi+dMyc* (90%, n=30), *ykiRNAi+CycE* (93.8%, n=32), *ykiRNAi+bsk*^{DN} (10%, n=30), and *ykiRNAi+Ets21cRNAi* (18.2%, n=33). (B) Percentage of wing discs with ACE: *GFP* (0%, n=28), *hpo+GFP* (96.8%, n=31), *wts+GFP* (76.5%, n=34), *Ets21c+GFP* (51.5%, n=33), *hep*^{CA}*+GFP* (77.4%, n=31), and *hep*^{CA}*+p35* (55.6%, n=36). (C) Percentage of wing discs with BCE (the wing discs used for this analysis are the same as those used in Fig. s3. A): *ykiRNAi+GFP* (100%, n=30), *ykiRNAi+p35* (74.2%, n=31), *ykiRNAi+ban* (16.7%, n=30), *ykiRNAi+diap1* (84.4%, n=32), *ykiRNAi+dMyc* (100%, n=30), *ykiRNAi+CycE* (100%, n=32), *ykiRNAi+bsk*^{DN} (10%, n=30) and *ykiRNAi+Ets21cRNAi* (60.6%, n=33). (D) Percentage of wing discs with BCE (the wing discs used for this analysis are the same as those used in Fig. s3. B): *GFP* (0%, n=28), *hpo+GFP* (100%, n=31), *wts+GFP* (100%, n=34), *hep*^{CA}*+GFP* (100%, n=31), and *hep*^{CA}*+p35* (100%, n=36). Results are shown as mean + SD. P values were calculated using two-tailed Student's t-test. *p < 0.05; **p < 0.01; ***p < 0.001; ****p < 0.0001; n.s., no significant difference.

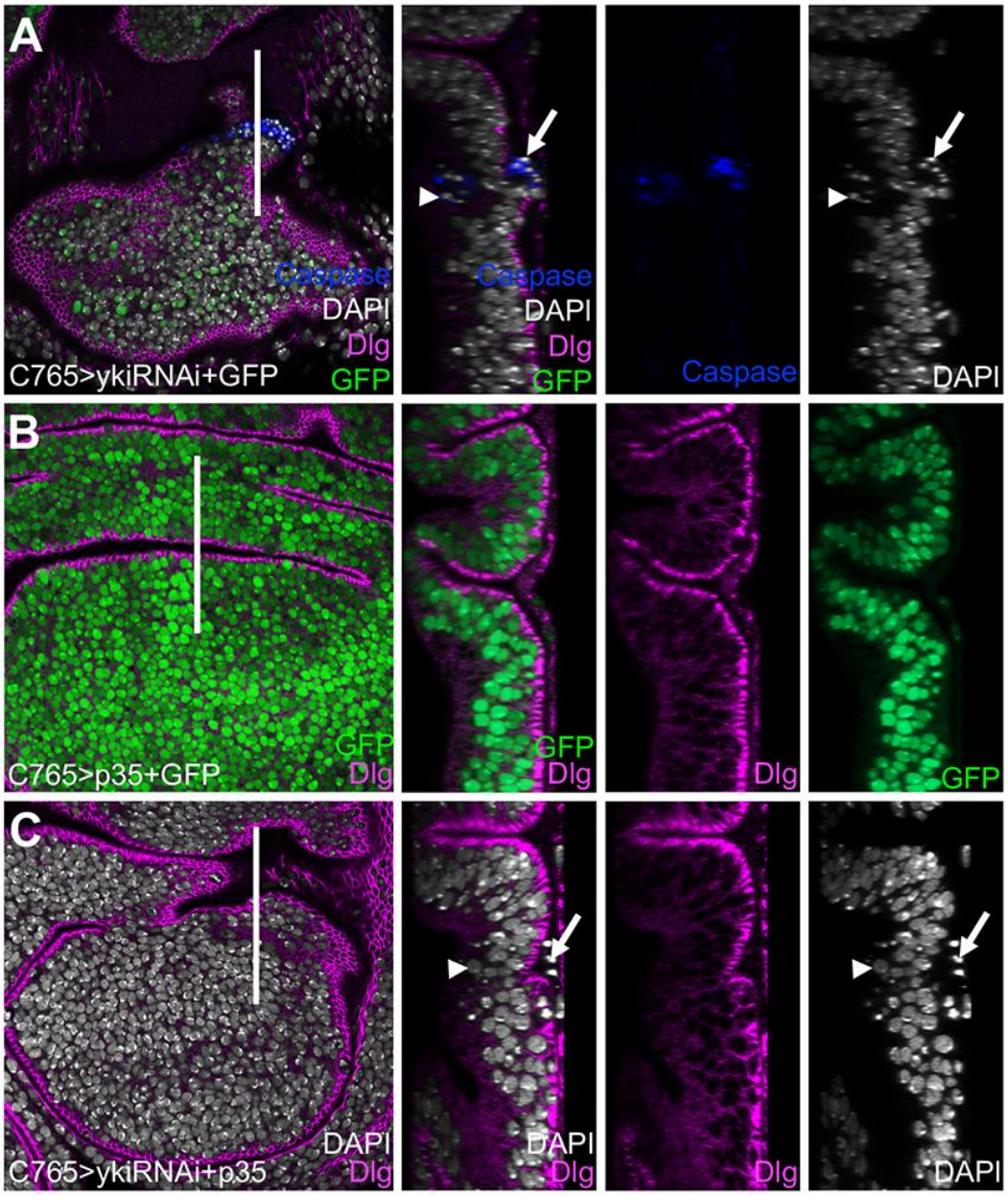

Figure S4. Suppressing apoptosis did not block *ykiRNAi* induced cell extrusion

(A) *ykiRNAi* induced cell extrusion and cleaved caspase-3 staining. (B) Control experiment, *p35* expression. (C) Co-expressing *p35* and *ykiRNAi* did not repress *ykiRNAi*-induced cell extrusion.

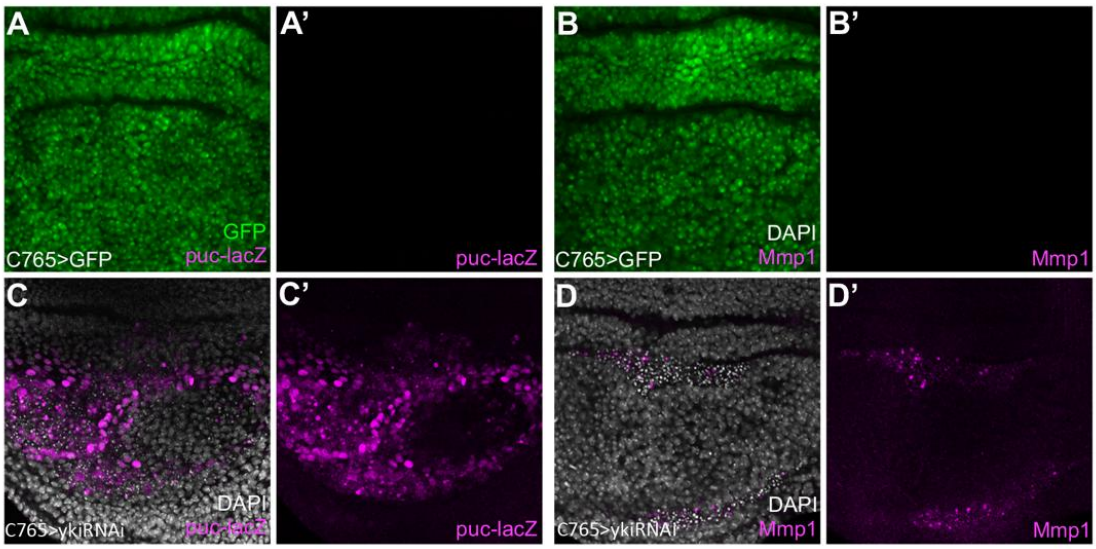

Figure S5. JNK signaling was activated in *ykiRNAi* expressing wing discs

puc (A') and *Mmp1* (B') were not expressed in control wing discs. (C and C') *puc* expression was activated in *ykiRNAi* expressing wing discs. (D, D') *Mmp1* expression was activated in *ykiRNAi* expressing wing discs.

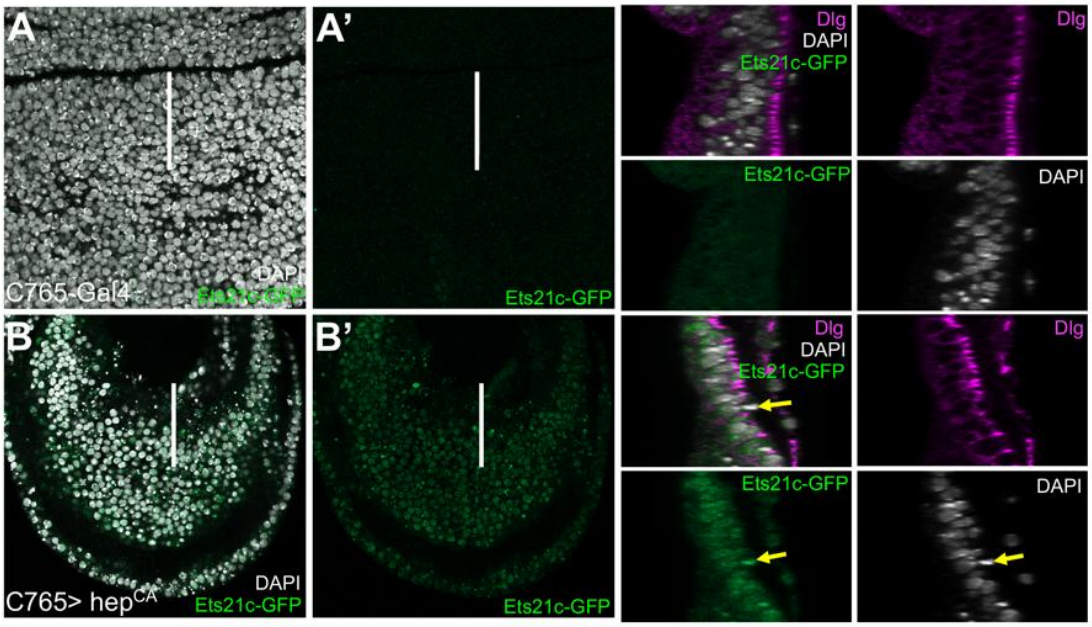

Figure S6. Ets21c-GFP level was increased when JNK signaling was activated

(A, A') *Ets21c-GFP* level is low in control wing discs. (B, B') Expression of hep^{CA} increased wing disc *Ets21c-GFP* levels including in the apically extruded cells (yellow arrow).

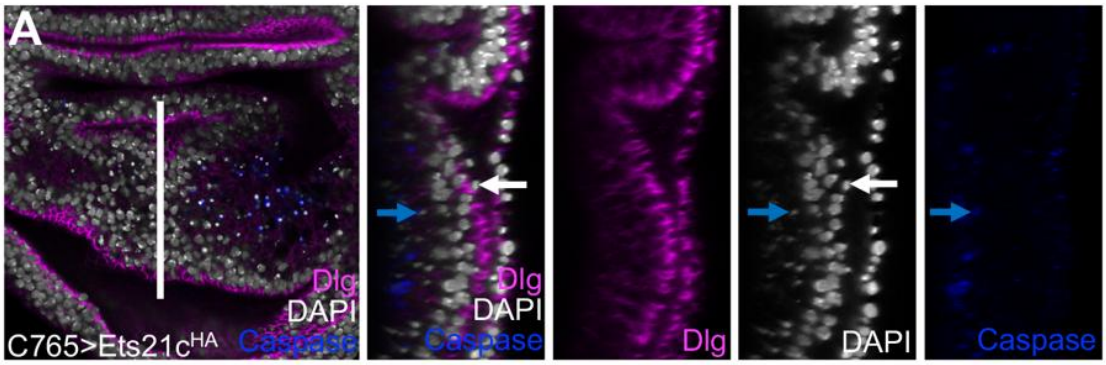

Figure S7. *Ets21c*-induced apical extruded cells were not undergoing apoptosis

(A) An x-y scan close to the basal section of the wing discs. Expression of *Ets21c*^{CA} induced apically extruded cells (arrow) with no cleaved caspase-3 staining. Most cleaved caspase-3 staining (blue arrow) was located on the basal side of the wing discs.

Table S1. Abundance of transcription of third instar larvae

Click here to Download Table S1

Table S2. Alterations in mRNA expression of 6 genes involved in Hpo pathway

genes	*Control*	*C765>ykiRNAi*	fold change	regulated
Act57B	17.06863333	30.011	1.591692872	up
Act87E	10.60510521	20.50697756	1.84484084	up
wgn	30.09160511	23.09001711	0.791146608	down
hth	13.89972479	8.764950015	0.710459822	down
ex	68.42301728	34.85187972	0.555330751	down
yki	67.43286075	18.55718096	0.304498467	down

Table S3. Selected genes subjected to quantitative RT-PCR

genes	*Control*	*C765>ykiRNAi*	fold change	regulated
hth	13.89972479	8.764950015	0.710459822	down
kmn1	63.83590667	26.65354333	0.427832717	down
puc	8.850264407	13.10390111	1.405928444	up
rpr	7.154933333	12.48833333	1.551257881	up
yki	67.43286075	18.55718096	0.304498467	down
Ets21c	0.436940337	1.458076081	2.026518117	up

Table S4. Primer sequences used for quantitative RT-PCR

hth-F	5'-CAAACCACCGGAGTTGGGAT-3'
hth-R	5'-AGGGGGTACTCACAACGTCT-3'
kmn1-F	5'-CCGCAGTGACGTACTGGAAT-3'
kmn1-R	5'-GTGCTTGCTTCATAGCGACG-3'
puc-F	5'-TTTCTGCTGACTTGCCACAC-3'
puc-R	5'-ATCCTCTCACACACTCGCTT-3'
rpr-F	5'-CGGGAGTCACAGTGGAGATT-3'
rpr-R	5'-TTTGGGTTTTGGGTTGGCTC-3'
yki-F	5'-GAGCAGGCAGTTACCGAGTC-3'
yki-R	5'-ACGCTAAGCCCAGATTGCAT-3'
Ets21c-F	5'-GTGCCAACAGAGGCCGATTA-3'
Ets21c-R	5'-CTGTTGGTGGGAACTTCCGT-3'
Actin-F	5'-CAGAGCAAGCGTGGTATCCT-3'
Actin-R	5'-CTCATTGTAGAAGGTGTGGTGC-3'

Table S5. Detailed genotypes for each figure

Click here to Download Table S5